

# **Impacts of Microwave Irradiation on the Physical and Chemical Characteristics of Virgin and PFOA-loaded Granular Activated Carbons**

*Yeakub Zaker<sup>†</sup>, Nazmiye Cemre Birben<sup>†</sup>, Habibullah Uzun<sup>†‡</sup>, Erica Gagliano<sup>§,&</sup>, Pietro P. Falciglia<sup>§</sup>, Paolo Roccaro<sup>§,\*</sup>, and Tanju Karanfil<sup>†\*</sup>*

<sup>†</sup>Department of Environmental Engineering and Earth Sciences, Clemson University, Anderson, SC 29625 USA

<sup>§</sup> Department of Civil Engineering and Architecture, University of Catania, Italy

<sup>&</sup> Department of Civil, Chemical and Environmental Engineering, University of Genoa, Italy

<sup>‡</sup> Department of Environmental Engineering, Marmara University, Istanbul, 34854 Turkey

\*Corresponding authors: tkaranf@clemson.edu; paolo.roccaro@unict.it

## ABSTRACT

Despite the worldwide application of adsorption through granular activated carbon (GAC), the regeneration of loaded GAC is still challenging particularly in presence of recalcitrant adsorbates such as poly- and perfluoroalkyl substances (PFAS). In this study, the impact of MW irradiation on the physical and chemical characteristics of virgin and PFOA-loaded coal-based granular activated carbons (GACs) was assessed at various MW irradiation conditions (i.e., time, MW power) for different particle size of GACs at dry (i.e., as received/processed) and wet (i.e., soaked in distilled deionized water, DDW) conditions. Temperatures above 600 °C were reached in three minutes at MW power  $\geq 250$  Watt regardless of GACs type (bituminous coal vs lignite coal), particle size, and GAC irradiation condition (dry vs wet). Faster temperature rise was attained for dry than wet GACs. Temperature increased up to 3x faster for small particles (20-40 mesh) than virgin (raw, as received) of both GACs regardless of the irradiation condition (dry vs wet). Upon MW irradiation, the changes in physical characteristics (i.e., surface area, pore volumes (i.e., total, micro, and meso), and % weight loss) of GACs were higher for lignite coal-based than bituminous coal-based GAC. However, the physical characteristics of GACs were not impacted due to the GAC particle sizes or irradiation conditions (dry or wet) after MW irradiation. Zero-point charge pH ( $\text{pH}_{\text{pzc}}$ ) increased towards more basic surfaces after MW irradiation. After ten (10) cycles of MW irradiation (at a temperature of 600-800 °C) of wet GAC samples, the variation of GAC surface area remained within 15%, while total and micropore volumes were within 22%. To understand the effect of multi-cycle MW irradiation on GAC characteristics in the presence of perfluoro octanoic acid (PFOA), 5-cyclic experiments (adsorption and successive MW regeneration) were conducted by using PFOA-loaded GAC in a surface water. The results

demonstrated no major impact of MW regeneration on the physical and chemical features of GACs, and the PFOA adsorption capacity (~100%) remained as compared to the raw carbon.

**Keywords:** Granular activated carbons, Microwave irradiation, GAC regeneration, PFOA

## 1. INTRODUCTION

Granular activated carbon (GAC) adsorption is commonly used in water treatment plants (WTPs) for the control of a variety of pollutants, such as synthetic organic contaminants (SOCs) [1-3], taste and odor (T&O) compounds [4], and dissolved natural organic matter (DOM) [5, 6]. In the past two decades, poly- and perfluoroalkyl substances (PFAS) – known as “forever chemicals”- have received increased attention worldwide due to their occurrence and persistence in different environmental media and their adverse health effects upon human exposure [7, 8]. As a result, the use of some long-chain compounds belonging to PFAS family [e.g., perfluorooctanoic acid (PFOA) and perfluoro octane sulfonic acid (PFOS)] was banned and/or subject to strict restrictions by regulatory agencies (e.g., US EPA, European Drinking Water Directive EU 2020/2184,) [7, 8]. Among different treatment alternatives (such as adsorption, photocatalysis, electro-Fenton oxidation, plasma treatment, and sono-chemical treatment), GAC adsorption has been one of the most economic and commonly used and effective process to remove PFAS from water in WTPs due to the suitability for the large-scale implementation and simple technology [3, 9, 10].

In full-scale WTPs, GAC in filters is periodically replaced when the breakthrough concentration levels for relevant pollutants are reached [3]. Spent GAC must be either (i) disposed of along with the adsorbed contaminants, or (ii) regenerated via thermal[11-13] or chemical techniques. It is more economical and preferable to regenerate and reuse the GAC than replacing it with the virgin GAC, as long as its adsorption capacity and physical characteristics are maintained after regeneration.

Microwave (MW) irradiation has been investigated as a potentially viable heat-based method for regenerating GACs exhausted with various adsorbates [14-19]. It was found to be a promising

alternative with reduced treatment time and energy consumption compared to conventional thermal regeneration [13]. MW dielectric heating is the primary mechanism involved in MW irradiation, which depends on the material's ability to absorb MW energy and convert it to heat [20-22]. MW heating takes advantage of GAC dielectric properties and the direct interactions between GAC delocalized  $\pi$ -electrons and microwaves [23-25]. Consequently, high heating rates, short treatment time, and potential energy-saving represent the key advantages of MW regeneration over conventional thermal treatment.

Systematic investigation for the effect of MW irradiation on the physical and chemical characteristics of GACs are very limited. Zhang et al. [26] investigated the impact of different MW power inputs (100-400 Watt (W)) on the surface area and pore size distribution of coal-based dry activated carbon (AC) samples with particle sizes in the ranges of 0.83-0.88 mm. They reported that the changes were within 15%, particularly a decrease in the Brunauer, Emmett, and Teller (BET) surface area and an increase in total pore volume ( $V_{\text{total}}$ ) and micro pore volume ( $V_{\text{micro}}$ ). Another study carried out for MW inputs power of 350 and 500 W for 60 min concluded that there was a little change (< 5%) in BET surface area,  $V_{\text{total}}$  and  $V_{\text{micro}}$  of a dry powder AC samples [27]. Ania et al. reported an increase of 6% in BET surface area of a commercially available coal-based dry AC sample (particle size ranges of 0.075-0.212 mm) exposed to MW irradiation at a temperature of 850 °C [28]. These two studies [28,29] focused on the effect of MW irradiation on dry carbons (i.e., with ambient moisture), and the applied MW power, irradiation temperature, and GAC particles sizes were distinctly different from each other.

The effect of MW irradiation on GAC adsorption and characteristics (BET surface area, pore volumes, zero-point charge pH ( $\text{pH}_{\text{pzc}}$ )) have also been partially reported in some other studies dealing with MW regeneration of GACs exhausted by organic or inorganic compounds (e.g.,

textile dyes, phenol, salicylic acid, toluene, sulfanilic acid, and various pharmaceutical compounds) [16, 17, 28-31]. Anionic acid blue dye adsorbed on a coconut based GACs did not impact the BET surface area and pore volumes after 4 cycles of MW regeneration at a temperature of  $\sim 300$  °C with a MW power of 200 W (variation  $< 5\%$ ) [16]. However, in the same study cationic basic blue dye-exhausted coconut shell based GACs showed  $\sim 35\%$  decrease in the BET surface area and pore volumes after 4 cycles of MW regeneration at the same temperature of  $\sim 300$  °C with a MW power of 200 W [16]. MW regeneration of sulfanilic acid exhausted coconut based GACs showed that the BET surface area of GAC decreased  $\sim 15\%$  in the presence of persulfate after 7 cycles of regeneration at 800 W for 1 min [31]. On the other hand, phenol exhausted coal based GACs showed to lose  $\sim 50\%$  of BET surface area and pore volumes after 6 cycles of MW regeneration under carbon dioxide ( $\text{CO}_2$ ) environment at a temperature of 850 °C [28]. Similar results to lose BET surface area and pore volumes was also reported for a textile dye exhausted agricultural waste based GACs after 5 cycles of MW regeneration at a MW power of 600 W for 2-3 min [30]. In some of these studies, pore width was reported to shift to a higher value with multiple cycles of MW regeneration [29-31], while  $\text{pH}_{\text{PZC}}$  was reported to increase due to MW treatment of various GAC [26, 28-30].

Overall, studies that thoroughly investigate the roles of multiple factors (such as MW power, irradiation time, GAC particle size, GAC irradiation condition (dry and wet), chemical nature (acidic vs. basic) and origin of GAC, and GAC temperatures) on the physical and chemical characteristics of GACs upon MW irradiations are limited in the literature. Therefore, we performed a systematic study to examine these factors. We treated one acidic mesoporous and one basic microporous activated carbon at two different particles size under both dry and wet conditions for different MW power and time with GACs reaching temperatures from 100 °C to

over 1000 °C. We extensively characterized the impacts of these treatment on GAC physical and chemical characteristics. We also conducted multi-cycles of MW irradiation for virgin and PFOA-loaded forms of these GACs to examine the impact of an organic adsorbate presence. PFOA was selected for these experiments due to its current practical significance as an emerging contaminant around the world [7, 8]. US EPA recently published a strategic roadmap for the treatment, remediation, destruction, disposal and mitigation of PFAS (PFOA is mentioned as one of the four to be considered) from solid and liquid medium [32]. Furthermore, we recently reported first MW regeneration of PFAS loaded GACs [13], thus, this is also part of our on-going efforts to understand the use of MW irradiation more comprehensively for the regeneration of PFAS-loaded GACs.

## 2. Materials and Methods

### 2.1 Materials

Two coal-based activated carbons, Calgon Filtrasorb 400 (F400) and Norit Hydrothermal 3000 (HD3000), which are commercially available and widely used in drinking water treatment plants (DWTPs)[3, 6] were used in the study. F400 is a microporous bituminous coal-based activated carbon with a high BET surface area and a basic  $\text{pH}_{\text{pzc}}$ , while HD3000 is mesoporous lignite coal-based activated carbon with a lower BET surface area and acidic  $\text{pH}_{\text{pzc}}$ . **Table S1** shows the measured surface area, porosity,  $\text{pH}_{\text{pzc}}$ , and ash content values for F400 and HD3000.

As-received virgin GAC samples were labelled as “R” (raw) and was used for MW irradiation and adsorption experiments in this study without any processing. To understand the role of GAC particle size, some raw GAC samples were crushed and sieved to obtain a particle size of 20-40 mesh size (0.425 – 0.850 mm), labelled as “P” (processed). Processed GACs were washed thoroughly with DDW and left overnight to settle in the large beakers in the DDW. Supernatant

water with carbon fines was decanted every day and the beaker was replenished with new DDW and settled again. This washing procedure was repeated for a week, and the GAC was finally dried overnight in an oven at 100 °C. Dried “P” GACs were stored in the desiccators until use.

GAC samples were also categorized as “dry” and “wet”, where “dry” is used for the GACs irradiated as it is obtained either as received (the moisture contents of “R” GAC were ~5 and ~10% for F400 and HD3000, respectively) or from the desiccator (the moisture content of “P” GAC was <1% for both) where it was stored and directly used in the experiments, and “wet” refers to the GAC was soaked in DDW (5 grams of GAC in 200 mL of DDW) for 24 hours, then vacuum filtered prior to the MW irradiation (the moisture contents were ~70 and ~90% for F400 and HD3000, respectively). Wet sample is to simulate GAC obtained from a fixed-bed adsorber at the field after removing the bulk water.

PFOA (CAS n. 335-67-1,  $\geq 98\%$  purity) purchased from TCI America. Liquid Chromatography (LC) grade water, methanol, and acetonitrile were acquired from Fischer Scientific. LC grade ammonium acetate and ammonium hydroxide were obtained from VWR Scientific. 18.2 M $\Omega$  (Type 1) DDW was used for all experiments.

## **2.2. Microwave irradiation experiments**

A commercially available 2.45 GHz - MW oven with a maximum power of 1.25 kW equipped with a cyclonic inverter was used for MW irradiation experiments. 5.0 g of GAC sample was placed in a ceramic crucible. Different power levels (125, 250, 375, and 500 W) and irradiation times (0-12 min) were set to perform MW irradiation. The final temperatures reached in GACs bed was measured using a K-type thermocouple (Omega Engineering Inc., U.S.A.). Afterwards, the GAC sample was transferred into a desiccator for cooling. The MW-irradiated GAC sample was characterized in terms of physical and chemical properties (e.g., % weight loss, BET surface

area, porosity, pH<sub>zpc</sub>, scanning electron microscopy (SEM) and ash content) to assess any changes due to MW irradiation.

The impact of multi-cycle MW irradiation has also been studied and characterized for wet GACs. For multiple-cycle MW irradiation experiments, cycles were carried out by sequential soaking of the GAC in DDW and MW irradiation of that wet GACs; this sequence was repeated ten times. MW irradiation of the GAC was carried out at a temperature of 600-800 °C, which was achieved by the MW power of 500 W and an irradiation time ~90 sec. Such high temperatures are specifically targeted to examine the resilience of GAC for removal of highly recalcitrant compounds such as PFOA belonging to PFAS family [12].

### **2.3. Adsorption and MW regeneration experiments of PFOA-loaded GACs for multiple cycles**

Multi-cycle MW regeneration of both raw GACs (F400 and HD3000) in the presence of PFOA was carried out with successive adsorption of 500 mg L<sup>-1</sup> PFOA either in DDW or a surface water (Lake Hartwell, South Carolina with 2.0 mg L<sup>-1</sup> of TOC, 0.026 cm<sup>-1</sup> of UV<sub>254</sub>, 2.7 mg L<sup>-1</sup> of chloride, 11.3 mg L<sup>-1</sup> of phosphate, and 17 mg L<sup>-1</sup> of alkalinity) followed by MW regeneration of wet PFOA-loaded GACs (at a temperature of 600-800 °C (500 W and ~90 sec)). In a typical adsorption experiment, 200 mL of 500 mg L<sup>-1</sup> PFOA solution was contacted with 5.0 g GAC sample for 72 hours in a shaker at a speed of ~200 rpm. The final mixture was vacuum filtered to collect the GAC and the filtrate. LC-MS/MS measurements were carried out to measure the PFOA concentrations as described in section 2.5. The amount of PFOA adsorbed by GACs was calculated as follows:

$$q = \frac{V(C_0 - C_f)}{m} \quad (1)$$

where  $q$  is the uptake ( $\text{mg g}^{-1}$ ),  $C_0$  ( $\text{mg L}^{-1}$ ) and  $C_f$  ( $\text{mg L}^{-1}$ ) are the initial and final concentrations of each compound in the solution, respectively, and  $V$  (L) is the volume of the solution and  $m$  (g) is the GAC mass.

For these experiments, the single-step desorption efficiency (SSDE, %) and overall regeneration efficiency (RE, %) were calculated as follows:

$$\text{SSDE} = \frac{q_n}{q_{n-1}} \cdot 100 \quad (2)$$

Where  $q_n$  and  $q_{n-1}$  are the uptakes of the MW regenerated GAC in a given cycle  $n$  and in the previous regeneration cycle ( $n-1$ ), respectively.

$$\text{RE} = \frac{q_i}{q_0} \cdot 100 \quad (3)$$

Where  $q_i$  is the uptake of the MW regenerated GAC and  $q_0$  is the uptake of the starting GAC samples.

#### 2.4. GAC characterization

GAC weight loss percentage (WL, %) represents a critical parameter for the applicability of a regeneration process. Weight loss was calculated as follows:

$$\text{WL} = \frac{w_0 - w_t}{w_0} \cdot 100 \quad (4)$$

Where  $w_0$  and  $w_t$  are the mass of GAC (g) before and after MW irradiation, respectively.

Before and after MW irradiation, GAC samples were analyzed with ASAP 2020 analyzer (Micromeritics Instrument Corp. U.S.) to determine the BET surface area and porosity (pore volumes and pore size distribution) by nitrogen physisorption data at 77 K after degassing the samples at 298 K for 10 h. The surface area was calculated by the BET equation, whereas a Density Functional Theory (DFT) model was used to determine the pore size distribution of GAC samples [5]. The reproducibility of measurements was assessed from duplicate data of randomly selected

samples and the relative standard deviation (RSD) of BET surface area, total pore volume ( $V_{\text{total}}$ ), micro pore volume ( $V_{\text{micro}}$ ), and meso pore volume ( $V_{\text{meso}}$ ) resulted in less than 5%.

The method for the measurement of  $\text{pH}_{\text{pzc}}$  was described in our previous publications [5]. Duplicate experiments were performed for randomly selected samples, and blanks with no carbon were also run with all samples. In brief, 0.1 M NaCl aqueous solutions were prepared using DDW, and the pH of the solutions was adjusted to the pH of 3.0, 5.0, 7.0, 9.0, and 11.0 by using 0.1 N HCl and/or NaOH solutions. 100 mg of GAC sample was soaked in 20 mL of these solutions in sealed vials and shaken for 48 h at 200 rpm at room temperature, and then left 24 h for settling of GAC. The final pH of the solution was measured. The  $\text{pH}_{\text{pzc}}$  was determined as the pH of the NaCl solution that did not vary after contact with the samples.

The ash content of the GAC samples was determined by using the ASTM D2866 method [33]. In brief, 100 mg of GAC sample (which was washed/sonicated with DDW, then dried at 105 °C and cooled the desiccator) was placed into a ceramic boat. Then, the boat was placed in a muffle furnace (Thermo Fisher Scientific) at 650 °C. After 16 hours, the boat was transferred into a desiccator for cooling to room temperature. The final mass of the boat with ash was measured. The duplicate of each sample was conducted simultaneously.

SEM imaging analyses were performed to examine the surface morphology, topography, and microstructure analysis of adsorbents. SEM images were measured using Hitachi SU9000 ultra-high resolution scanning electron microscope. Hitachi SU9000 has a resolution of 0.4 nm at 30 kV. Initially, sample preparation was performed by mounting specimens on 4 mm x 10 mm mounts using double side adhesive carbon tape. The surfaces of the specimen were cleaned for 3 min by using a vacuum UV cleaner to remove surface contaminants before imaging. The microscope was operated at an acceleration voltage range of 5-15 kV and filament emission current of 10 mA.

Images were captured with secondary electron (SE) in a lens detector at 500k magnification. Elemental analysis of surfaces in SEM is performed by using energy dispersive spectroscopy (EDS) which was carried out with Oxford Instruments Ultim Max detector. K-alpha lines for C, N, O, and S at an electron beam energy of 10 kV were measured to perform atomic composition analysis.

## **2.5. PFOA analysis**

The determination of PFOA in water samples was conducted according to the US EPA method 533 with few modifications [34]. Specifically, the high-volume direct injection was performed using a Liquid Chromatography coupled to ESI-triple Quadrupole Mass Spectrometer (Agilent 6470 LC/TQ) operated in the negative ionization mode. The mobile phase solvents were 100 mM ammonium acetate/ammonium hydroxide in water (pH 10) (solution A), and acetonitrile (solution B). A combination of 50% of A and 50% of B was delivered at a flow rate of 0.4 mL min<sup>-1</sup> by the binary pump containing an Agilent ZORBAX RRHD Eclipse Plus C18 column (2.1 × 100 mm, 1.8 μm particle size). Polytetrafluoroethylene-free vials, caps, and pipet tips (sterile) were used to reduce PFAS background. Multiple Reaction Monitoring (MRM) mode was used for data acquisition. Two MRM transitions (PFOA: 413/169, 413/369) were used for quantification and confirmation, respectively.

Before analysis, samples were diluted with LC-grade water to obtain PFOA concentrations ranging between 0.5 and 100 μg L<sup>-1</sup>. Afterward, calibration curves were constructed and the correlation coefficients (R<sup>2</sup>) of the calibration curves for PFOA was >0.99. Based on the lowest acceptable calibration standard, the detection limit of PFOA measurements was 0.5 μg L<sup>-1</sup>.

## **3. Results and Discussion**

### **3.1 Temperature profiles of GAC samples under various MW power and irradiation time**

**Figure 1** shows the temperature profiles of F400 GACs (R and P) as a function of irradiation times for different MW powers (125 W, 250 W, 375 W, and 500 W), and the linear regressions for the data. Similar data for HD3000 GACs are shown in **Figure S1**. The calculated temperature increase rates of both GACs are shown in **Table S2**. MW irradiation led to an increase in GAC temperatures, while the rate of temperature increase decreased with decreasing MW power. The temperature of GACs exceeded 600 °C in 3 minutes with a MW power over 250 W, regardless of GACs type (F400 vs. HD3000), particle size (0.850 - 2.000 mm (R) vs. 0.425 - 0.850 mm (P)), and moisture level (dry vs. wet). Similarly, in a previous study, GAC temperature reached over 600 °C in 3 minutes with a MW power of 300 W or higher for a coal-based GAC [26]. The temperature rise during MW irradiation was attributed to the ability of GAC to absorb MW energy (i.e., dielectric properties), which depends on the nature of the carbon (origin, particle size, etc.), moisture content (dry and wet) as well as the applied MW power [26, 35, 36].

For all GAC samples, faster temperature increases were observed under the dry conditions than wet ones, as indicated by the higher slopes of the temperature profiles (**Table S2**). The presence of water has the ability to increase the dielectric properties of the porous medium, and eventually MW penetration and the heating of the entire medium [23]. Moreover, an excess amount of water may turn the system into endothermic conditions, increasing the energy required to reach the desired temperatures. In general, MW activation occurs faster in dry than wet GACs [36].

The temperature increases at a faster rate for smaller than larger particules (F400 P vs. F400 R (Figure 1A-B), HD3000 P vs. HD3000 R (Figure S1A-B)). This was attributed to the more uniformity, better heat conductivity, and lower MW reflection of the smaller particles, thus transforming MW energy to thermal energy, and resulting in higher final temperature values [37]. It has been previously reported that under similar experimental conditions, larger size particles

displayed lower devolatilization rates due to lower particle temperature as a result of the decrease of heat transfer between the particle and the heating source [38, 39].

The temperature of HD3000 (lignite coal-based mesoporous acidic GAC) was found to increase faster than F400 (bituminous coal-based microporous GAC), regardless of particle size or moisture content, which was attributed to the ash and oxygen contents of the GACs. HD3000 has higher ash (11.6%) and oxygen (8.7%) contents than the F400 (7.5% of ash and 5.9% of oxygen), see **Table S1**).

### **3.2 The effect of MW irradiation on physical and chemical characteristics of GAC samples**

The results of physical and chemical characterization of F400 and HD3000 GAC samples before and after MW irradiation are discussed in this section. GACs were exposed to different MW powers for different times and the temperatures reached were measured. The temperature-dependent changes of the physical (BET surface area,  $V_{\text{total}}$ ,  $V_{\text{micro}}$ ,  $V_{\text{meso}}$ , and % wet loss) and chemical ( $\text{pH}_{\text{pzc}}$  and ash content) characteristics of the GAC samples were presented in **Figures 2-5 and S2-4**.

#### **3.2.1 The effect on the GAC physical characteristics**

The temperature-dependent BET surface area profiles of GAC samples (R and P) after MW irradiation are reported in **Figure 2**. The changes in BET surface area remained within  $\pm 8$ -15% for both GACs compared to the untreated samples independent of the temperature, GACs type, particle size, and wet vs. dry (see **Table 1**). Therefore, the effect of the MW irradiation on the surface areas of the samples was small ( $P < 0.05$ ) regardless of particle sizes or dry or wet conditions. In three previous studies with coal-based dry AC, it has been reported that the change in BET surface area as a result of MW irradiation remained within 15% [26-28].

The temperature dependent  $V_{\text{total}}$ ,  $V_{\text{micro}}$ , and  $V_{\text{meso}}$  profiles of GAC samples before and after MW irradiation are reported in **Figures S2-4**, respectively, and analyses are reported in Table 1. It was observed that GAC types played an important role in the changes of the  $V_{\text{total}}$ ,  $V_{\text{micro}}$ , and  $V_{\text{meso}}$  changes for GAC samples. Bituminous coal-based F400 GAC showed more stability during MW irradiation than lignite coal-based HD3000 for those properties. F400 GAC showed 7-10, 4-9, and 21-38% of changes in  $V_{\text{total}}$ ,  $V_{\text{micro}}$ , and  $V_{\text{meso}}$ , respectively, compared to the untreated GAC samples. It was noted that  $V_{\text{meso}}$  of virgin F400 was  $\sim 0.05 \text{ cm}^3/\text{g}$ , therefore, small fluctuation in  $V_{\text{meso}}$  showed high percentage of changes. On the other hand, HD3000 GAC showed changes of 10-18, 16-22, and 21-29% for  $V_{\text{total}}$ ,  $V_{\text{micro}}$ , and  $V_{\text{meso}}$ , respectively, compared to the untreated GAC samples. However, other GAC properties (particle size, and moisture contents (dry vs. wet)) did not affect  $V_{\text{total}}$ ,  $V_{\text{micro}}$ , and  $V_{\text{meso}}$  during MW irradiation. Our results collectively with the previous studies [28-30] indicates that the changes in BET surface area of coal-based GAC samples were relatively small ( $<15\%$ ), while the decrease in the pore volumes of lignite coal-based GACs by MW irradiation were higher than bituminous coal-based GAC.

The temperature-dependent weight loss profiles of GAC samples after MW irradiation are reported in **Figure 3**. The weight loss from both “R” GAC samples was significantly higher (5-11% for F400 R and 10-18% for HD3000 R) than “P” GAC samples (0-8% for F400 P and HD3000 P) even at a lower temperature regardless of the wet or dry condition. Raw (R) samples were irradiated as received with no processing, while “P” was washed several times after crushing and sieved before the irradiation. It appears that some impurities were removed during both washing and increasing temperature. It has been reported that lower reaction temperatures may cause lower weight losses due to incomplete removal of the volatiles in GACs [40]. These impurities are likely in organic origin as the ash content analysis, to be discussed later, did not show a major difference

between R and P. With increasing temperature, weight loss increased for all GACs samples, indicating carbon burn off, removal functional groups via decomposition. With offsetting the moisture content (Table 1), it was found that the weight loss increased by 3-6 and 6-8% for F400 and HD3000 GACs, respectively. Therefore, there were no extra impact for both GAC in weight loss from the particle size, processing, and wet vs dry conditions. Previously, the modification of a GAC by conventional heating (650, 800, and 950 °C) under H<sub>2</sub> atmosphere showed an increase in weight loss from 12.6 to 20.2% as the temperature was increased from 650 to 950 °C [41]. Thermal degradation profiles of GAC samples under nitrogen atmosphere and heating rate of 25 K/min using thermo-gravimetric analysis curves resulted in 11% of weight losses in the temperature range of 100-1000 °C [42].

### 3.2.2 The impact on chemical characteristics of GAC samples

The temperature-dependent pH<sub>pzc</sub> profiles of GAC samples after MW irradiation are provided in **Figure S5**. The pH<sub>pzc</sub> value of basic F400 GAC samples increased about one pH unit, whereas the pH<sub>pzc</sub> value of acidic HD3000 GAC samples increased about five pH units with increasing temperature regardless of particles size and dry vs. wet conditions. A strong correlation ( $R^2 > 0.75$ ) was observed between the temperature and pH<sub>pzc</sub> (Figure S5). Carboxyl, lactone, phenol, carbonyl and quinone are some of the surface functional groups that have been identified on AC surfaces [43, 44]. Upon exposure to high temperatures, these surface functional groups tend to decompose according to their thermal stabilities, and the carbon surface becomes more basic [26, 44-46]. MW irradiations were also reported to increase the pH<sub>pzc</sub> values of coal-based GAC samples with increasing temperature [24, 27, 28, 46].

The temperature-dependent ash content profiles of GAC samples after MW irradiation are shown in **Figure S6** and increase of ash content from untreated GAC samples are presented in

Table 1. The increase in the ash content with temperature was 1% for F400 GACs (ash content of untreated F400 is 7.5%, Table S1), while it increased 2-7% for HD3000 GAC (ash content of untreated HD3000 is 11.7%, Table S1) samples under both dry and wet MW irradiation conditions. The ash content of HD3000 increased more than F400 upon MW irradiation which was attributed to the higher weight losses observed for the HD3000 GACs. The higher degree of removal of organic than inorganic components from carbon with temperature can be the reason for the observed change in ash content. Generally, organic functional groups, like carboxyl, lactone, phenol, carbonyl and quinone, which are known to present in the surface of the AC [43, 44] are known to decompose quickly at low temperatures ( $\leq 300$  °C). On the other hand, the inorganic component in the AC surface consists of inorganic oxides ( $\text{SiO}_2$ ,  $\text{Al}_2\text{O}_3$ , etc.) are very stable even at high temperature ( $\approx 1000$  °C).

### **3.3. The effect of multi-cycle MW irradiation on physical and chemical characteristics of GAC samples**

The effect of multi-cycle MW irradiation on physical and chemical characteristics of F400 (R and P) and HD3000 (R and P) samples were assessed in terms of GAC temperature, % weight loss, BET surface area,  $V_{\text{total}}$ ,  $V_{\text{micro}}$ ,  $V_{\text{meso}}$ , and elemental compositions (by SEM-EDS). MW regenerated GACs were characterized after the 1<sup>st</sup>, 5<sup>th</sup>, and 10<sup>th</sup> cycle of MW regeneration. Results for F400 (R and P) GAC samples were presented in **Figure 4** and SEM images of F400 R samples are shown in **Figure 5**. Results for HD3000 (R and P) GAC samples are presented in **Figure S7** and SEM images of HD3000 R samples are shown in **Figure S8**. SEM-EDS elemental compositions (C, O, N, and S) and pH<sub>pzc</sub> of virgin and MW irradiated F400 R and HD3000 R GACs after 1<sup>st</sup>, 5<sup>th</sup>, and 10<sup>th</sup> cycle are shown in **Table S3**.

Weight loss profiles revealed the highest weight loss occurred during the first cycle (~7% for F400 R, ~4% for F400 P, ~17% for HD3000 R, and ~6% for HD3000 P) of MW irradiation and then remained relatively constant (<2% for both samples) for ten MW irradiation cycles. After 10<sup>th</sup> successive cycles of MW irradiation, cumulative weight losses were 17% (F400 R), 12% (F400 P), 25% (HD3000 R), and 18% (HD3000 P). The BET surface area,  $V_{\text{total}}$ ,  $V_{\text{micro}}$ , and  $V_{\text{meso}}$  of both GACs increased in the ranges of 10-15% regardless of particle sizes for both GACs. The microporous nature of F400 and the mesoporous nature of HD3000 are visible in the SEM images. SEM images show several small pores on the GAC surfaces with no visible impact from the multiple cycles of MW irradiation. SEM-EDS analyses showed that the changes in elemental composition, % weight of carbon, oxygen, nitrogen, and sulfur, were the highest during the 1<sup>st</sup> cycle of MW irradiation for both GAC (See **Table S3**). For F400 GAC, carbon composition increased by 4.1%, whereas oxygen and sulfur compositions decreased by 2.3 and 0.2%, respectively, and nitrogen compositions remain same. For HD3000 GAC, carbon composition increased by 2.4% whereas oxygen, nitrogen, and sulfur compositions decreased by 4.9, 0.1, and 0.6%, respectively. The changes in elemental compositions after the fifth and tenth cycles of MW irradiation were relatively small in compared the changes after the first cycle of MW irradiation. These changes are correlated with changes in the  $\text{pH}_{\text{pzc}}$  (see section 3.2 Figure S5 and Table S3); the first cycle of MW irradiation resulted in a more basic surface of the GACs over a temperature of 600 °C, also decreasing the oxygen and sulfur contents. Overall, these experiments showed that at temperature ranging from 600 to 800 °C, there was insignificant impacts ( $P < 0.05$ ) on GAC physical characteristics (BET surface area,  $V_{\text{total}}$ ,  $V_{\text{micro}}$ , and  $V_{\text{meso}}$ ) which is also confirmed by the SEM images in Figures 5 and S8. However, GAC surface became more basic.

### 3.4. Multi-cycle MW regeneration of PFOA-loaded GACs in a surface water

Although multi-cycle MW irradiation in wet (i.e., soaked in DDW) condition (temperatures of ~600-800 °C) did not significantly impacted the physical characteristics (BET surface area,  $V_{total}$ ,  $V_{micro}$ , and  $V_{meso}$ ) of both GACs (F400 and HD3000) as discussed in the previous section, it was important to further confirm these findings for GACs loaded in natural waters with both organic and inorganic components. Therefore, both GACs were loaded with PFOA (20 mg/g GAC) in a surface water. The GACs were then treated with MW irradiation and characterized in terms of temperature, % weight loss, BET surface area,  $V_{total}$ ,  $V_{micro}$ , and  $V_{meso}$ , GAC elemental compositions, PFOA uptake on GAC, PFOA RE, and PFOA SSDE. They are presented in **Figures 6 and 7**, and **Table S4**. The SEM images are shown in **Figure S9**.

Adsorption of PFOA reduced the BET surface area and pore volumes by ~15 to 20% as compared to the virgin GAC samples (**Figure 6**). SEM-EDS analyses showed ~3% of fluorine (F) weight percent on the surface of GACs, which was absent on the virgin GAC (**Table S4**), and SEM images also indicate less porous surfaces of GACs (**Figure S9**) as compared to the virgin GACs (**Figures 7 and S6**). Multi-cycle MW regeneration almost completely restored the BET surface area and pore volumes within 5 to 10% difference as compared to the virgin GAC (**Figure 8**). Thus, MW irradiation at temperatures of 600-800 °C, which was achieved by the MW power of 500 W and an irradiation time ~90 sec, effectively removed PFOA from the pores of GACs, and there was no permanent impact on the GAC physical characteristics by the presence of PFOA and the components of the surface water (NOM and inorganic components) during multi-cycle MW regeneration. PFOA uptake of both GACs did not change with the multiple cycles of MW regeneration. The RE and SSDE were ~100% even after the 5<sup>th</sup> cycle of MW regenerations of both GACs in DDW and the surface water (**Figure 7**). Weight loss profiles were similar to those without

PFOA experiments (Figures 4A and S7A). This indicated that PFOA and the surface components did not alter the PFOA uptake and weight loss profile of GACs. Therefore, these findings pointed out the promising nature of multicycle MW irradiation for GAC regeneration at high temperatures for recalcitrant compounds like PFAS. The fate of PFOA during MW irradiation is not the focus in this paper, and it is being investigated in detail along with other PFAS compounds and background water quality conditions, which will be discussed in future publications.

#### 4. Conclusions

The impact of MW irradiation on GAC samples was extensively assessed by investigating the changes in physical and chemical properties after irradiation performed at different power, time, successive cycles, and GAC features (wet vs. dry, particle size, virgin vs. PFOA-loaded). The main findings from this work are as follows:

- MW irradiation increased the temperature of GACs rapidly above 600 °C in a relatively short irradiation time (~three minutes) with a MW power  $\geq 250$  W for both GACs tested in this study, two particle sizes, and dry and wet conditions.
- The changes in BET surface areas of bituminous coal based F400 GAC samples were relatively small, while the decrease in the pore volumes of lignite coal based HD3000 GACs by MW irradiation were higher than F400. The  $\text{pH}_{\text{pzc}}$  value of basic F400 GAC samples increased about one pH unit, whereas the  $\text{pH}_{\text{pzc}}$  value of acidic HD3000 GAC samples increased about five pH units with increasing temperature independent of particles size and dry vs. wet conditions.
- Weight loss profiles of multi-cycle MW irradiation experiments revealed the highest weight loss occurred during the first cycle. After 10<sup>th</sup> successive cycles of MW

irradiation, cumulative weight losses were 17% (F400 R), 12% (F400 P), 25% (HD3000 R), and 18% (HD3000 P). The BET surface area,  $V_{\text{total}}$ ,  $V_{\text{micro}}$ , and  $V_{\text{meso}}$  of both GACs increased in the ranges of 10 – 15% regardless of particle sizes for both GACs.

- Multi-cycle MW regeneration (at temperatures of 600-800 °C, which was achieved by the MW power of 500 W and an irradiation time ~90 sec) of PFOA loaded GACs in a surface water almost completely restored the BET surface area and pore volumes within 5 to 10% difference as compared to the virgin GAC, effectively removing PFOA from the pores of GACs, and with no permanent impact on the GAC physical characteristics. PFOA uptake of both GACs did not change with the 5 cycles of MW regeneration/adsorption, indicating that PFOA and the surface components did not alter the POA uptake and weight loss profile of GACs.

Overall, MW irradiation did not impact the main characteristics of the GACs (BET surface area, pore volumes) especially for the bituminous coal-based GAC after multiple cycle of MW irradiation experiments. The findings support MW technology as a promising technology to apply for the regeneration of spent GACs (and reuse) in the drinking water treatment for different organic contaminants and background natural organic matter.

## **ACKNOWLEDGMENTS**

The study was supported by a research grant from the Water Research Foundation (Project 5103). However, the manuscript has not been subjected to peer and policy review of the agency and therefore, does not necessarily reflect its views.

## REFERENCES

- [1] O.S. Arvaniti, A.S. Stasinakis, Review on the occurrence, fate and removal of perfluorinated compounds during wastewater treatment, *Sci. Total Environ.*, 524-525 (2015) 81-92.
- [2] M. Park, S. Wu, I.J. Lopez, J.Y. Chang, T. Karanfil, S.A. Snyder, Adsorption of perfluoroalkyl substances (PFAS) in groundwater by granular activated carbons: Roles of hydrophobicity of PFAS and carbon characteristics, *Water Res.*, 170 (2020) 115364.
- [3] D. Gonzalez, K. Thompson, O. Quiñones, E. Dickenson, C. Bott, Granular activated carbon-based treatment and mobility of per-and polyfluoroalkyl substances in potable reuse for aquifer recharge, *AWWA Water Sci.*, 3 (2021) e1247.
- [4] M. Drikas, M. Dixon, J. Morran, Removal of MIB and geosmin using granular activated carbon with and without MIEX pre-treatment, *Water Res.*, 43 (2009) 5151-5159.
- [5] S.A. Dastgheib, T. Karanfil, W. Cheng, Tailoring activated carbons for enhanced removal of natural organic matter from natural waters, *Carbon*, 42 (2004) 547-557.
- [6] T. Karanfil, Activated carbon adsorption in drinking water treatment, *Interface Sci. Technol.* (2006) 345-373.
- [7] U. S. EPA, Drinking Water Health Advisory for Perfluorooctanoic Acid (PFOA), EPA Document 822-R-16-005, (2016).
- [8] European Parliament and the Council, Official Journal of the European Union, (2020).
- [9] I. Ross, J. McDonough, J. Miles, P. Storch, P. Thelakkat Kochunarayanan, E. Kalve, J. Hurst, S. S. Dasgupta, J. Burdick, A review of emerging technologies for remediation of PFASs, *Remed. J.*, 28 (2018) 101-126.

- [10] B. Ji, P. Kang, T. Wei, Y. Zhao, Challenges of aqueous per-and polyfluoroalkyl substances (PFASs) and their foreseeable removal strategies, *Chemosphere*, 250 (2020) 126316.
- [11] F. Xiao, P.C. Sasi, B. Yao, A. Kubátová, S.A. Golovko, M.Y. Golovko, D. Soli, Thermal stability and decomposition of perfluoroalkyl substances on spent granular activated carbon, *Environ. Sci. Technol. Lett.*, 7 (2020) 343-350.
- [12] N. Watanabe, M. Takata, S. Takemine, K. Yamamoto, Thermal mineralization behavior of PFOA, PFHxA, and PFOS during reactivation of granular activated carbon (GAC) in nitrogen atmosphere, *Environ. Sci. Pollut. Res.*, 25 (2018) 7200-7205.
- [13] E. Gagliano, P.P. Falciglia, Y. Zaker, T. Karanfil, P. Roccaro, Microwave regeneration of granular activated carbon saturated with PFAS, *Water Res.*, 198 (2021) 117121.
- [14] C. Ania, J. Parra, J. Menendez, J. Pis, Microwave-assisted regeneration of activated carbons loaded with pharmaceuticals, *Water Res.*, 41 (2007) 3299-3306.
- [15] C.O. Ania, J.B. Parra, J.A. Menéndez, J.J. Pis, Effect of microwave and conventional regeneration on the microporous and mesoporous network and on the adsorptive capacity of activated carbons, *Microporous Mesoporous Mater.*, 85 (2005) 7-15.
- [16] G. Durán-Jiménez, L.A. Stevens, G.R. Hodgins, J. Uguna, J. Ryan, E.R. Binner, J.P. Robinson, Fast regeneration of activated carbons saturated with textile dyes: Textural, thermal and dielectric characterization, *Chem. Eng. J.*, 378 (2019) 121774.
- [17] P.P. Falciglia, E. Gagliano, V. Brancato, G. Finocchiaro, A. Catalfo, G. De Guidi, S. Romano, P. Roccaro, F.G.A. Vagliasindi, Field technical applicability and cost analysis for microwave based regenerating permeable reactive barriers (MW-PRBs) operating in Cs-contaminated groundwater treatment, *J. Environ. Manage.*, 260 (2020) 110064.

- [18] P.P. Falciglia, E. Gagliano, V. Brancato, G. Malandrino, G. Finocchiaro, A. Catalfo, G. De Guidi, S. Romano, P. Roccaro, F.G.A. Vagliasindi, Microwave based regenerating permeable reactive barriers (MW-PRBs): Proof of concept and application for Cs removal, *Chemosphere*, 251 (2020) 126582.
- [19] F.K. Yuen, B. Hameed, Recent developments in the preparation and regeneration of activated carbons by microwaves, *Adv. Colloid Interface Sci.*, 149 (2009) 19-27.
- [20] A. Zlotorzynski, The application of microwave radiation to analytical and environmental chemistry, *Crit Rev Anal Chem*, 25 (1995) 43-76.
- [21] D. Stuerger, P. Gaillard, Microwave Athermal Effects in Chemistry: A Myth's Autopsy: Part I: Historical background and fundamentals of wave-matter interaction, *J. Microw. Power Electromagn. Energy*, 31 (1996) 87-100.
- [22] D. Stuerger, M. Delmotte, Wave-material interactions, microwave technology and equipment, *Microwaves in organic synthesis*, (2002) 1-33.
- [23] P.P. Falciglia, P. Roccaro, L. Bonanno, G. De Guidi, F.G.A. Vagliasindi, S. Romano, A review on the microwave heating as a sustainable technique for environmental remediation/detoxification applications, *Renew. Sust. Energ. Rev.*, 95 (2018) 147-170.
- [24] J.V. Nabais, P. Carrott, M.R. Carrott, J. Menéndez, Preparation and modification of activated carbon fibres by microwave heating, *Carbon*, 42 (2004) 1315-1320.
- [25] O. Zanella, I.C. Tessaro, L.A. Féris, Desorption-and decomposition-based techniques for the regeneration of activated carbon, *Chem. Eng. Technol.*, 37 (2014) 1447-1459.
- [26] L. Zhang, M. Mi, B. Li, Y. Dong, Modification of activated carbon by means of microwave heating and its effects on the pore texture and surface chemistry, *Res. J. Appl. Sci. Eng. Technol*, 5 (2013) 1836-1840.

- [27] E. Çalışkan, J. Bermúdez, J. Parra, J. Menéndez, M. Mahramanlioğlu, C. Ania, Low temperature regeneration of activated carbons using microwaves: Revising conventional wisdom, *J. Environ. Manage.*, 102 (2012) 134-140.
- [28] C.O. Ania, J.A. Menéndez, J.B. Parra, J.J. Pis, Microwave-induced regeneration of activated carbons polluted with phenol. A comparison with conventional thermal regeneration, *Carbon*, 42 (2004) 1383-1387.
- [29] X. Quan, X. Liu, L. Bo, S. Chen, Y. Zhao, X. Cui, Regeneration of acid orange 7-exhausted granular activated carbons with microwave irradiation, *Water Research*, 38 (2004) 4484-4490.
- [30] K. Foo, Effect of microwave regeneration on the textural network, surface chemistry and adsorptive property of the agricultural waste based activated carbons, *Process Saf. Environ. Prot.*, 116 (2018) 461-467.
- [31] M.-C. Wei, K.-S. Wang, I.-C. Lin, T.-E. Hsiao, Y.-N. Lin, C.-T. Tang, J.-C. Chen, S.-H. Chang, Rapid regeneration of sulfanilic acid-sorbed activated carbon by microwave with persulfate, *Chem. Eng. J.*, 193 (2012) 366-371.
- [32] U. S. EPA, PFAS Strategic Roadmap, 2021.
- [33] A.D.-. ASTM, Standard Test Method for Total Ash Content of Activated Carbon. , ASTM Int., (2018).
- [34] U. S. EPA, Method 533, 2019.
- [35] J. Menéndez, E. Menéndez, A. Garcia, J. Parra, J. Pis, Thermal treatment of active carbons: A comparison between microwave and electrical heating, *Microw. Power Electromagn. Energy*, 34 (1999) 137-143.

- [36] X. Liu, X. Quan, L. Bo, S. Chen, Y. Zhao, Simultaneous pentachlorophenol decomposition and granular activated carbon regeneration assisted by microwave irradiation, *Carbon*, 42 (2004) 415-422.
- [37] H. Li, Z. Zhao, C. Xiouras, G.D. Stefanidis, X. Li, X. Gao, Fundamentals and applications of microwave heating to chemicals separation processes, *Renew. Sust. Energ. Rev.*, 114 (2019) 109316.
- [38] Y. Shuang, C. Wu, B. Yan, Y. Cheng, Heat transfer inside particles and devolatilization for coal pyrolysis to acetylene at ultrahigh temperatures, *Energy Fuels*, 24 (2010) 2991-2998.
- [39] B. Tian, Y.y. Qiao, Y.y. Tian, Q. Liu, Investigation on the effect of particle size and heating rate on pyrolysis characteristics of a bituminous coal by TG–FTIR, *J. Anal. Appl. Pyrolysis*, 121 (2016) 376-386.
- [40] T. Chen, H. Liu, R. Bie, Temperature rise characteristics of coal-KOH adduct under microwave heating and the properties of resultant activated carbon for catalytic methane decomposition, *J. Anal. Appl. Pyrolysis*, 145 (2020) 104739.
- [41] J.A. Menéndez, J. Phillips, B. Xia, L.R. Radovic, On the modification and characterization of chemical surface properties of activated carbon: in the search of carbons with stable basic properties, *Langmuir*, 12 (1996) 4404-4410.
- [42] D. Grekov, P. Pré, B.J. Alappat, Microwave mode of heating in the preparation of porous carbon materials for adsorption and energy storage applications—An overview, *Renew. Sust. Energ. Rev.*, 124 (2020) 109743.
- [43] S. Biniak, G. Szymański, J. Siedlewski, A. Świątkowski, The characterization of activated carbons with oxygen and nitrogen surface groups, *Carbon*, 35 (1997) 1799-1810.

- [44] J.L. Figueiredo, M. Pereira, M. Freitas, J. Orfao, Modification of the surface chemistry of activated carbons, *Carbon*, 37 (1999) 1379-1389.
- [45] P. Carrott, J. Nabais, M.R. Carrott, J. Menéndez, Thermal treatments of activated carbon fibres using a microwave furnace, *Microporous Mesoporous Mater.*, 47 (2001) 243-252.
- [46] X. Ge, F. Tian, Z. Wu, Y. Yan, G. Cravotto, Z. Wu, Adsorption of naphthalene from aqueous solution on coal-based activated carbon modified by microwave induction: Microwave power effects, *Chem. Eng. Process.: Process Intensif.*, 91 (2015) 67-77.

**Table 1.** The maximum changes in the physical and chemical characteristics of F400 GAC samples after MW irradiation.

Sample	$\Delta$ BET surface area	$\Delta$ Total pore volume	$\Delta$ Micropore volume	$\Delta$ Mesopore volume	$\uparrow$ Weight loss	$\Delta$ pH <sub>pzc</sub>	$\uparrow$ Ash content
F400 R dry	$\pm 10\%$	$\pm 8\%$	$\pm 4\%$	$\pm 21\%$	3%	+10%	1%
HD3000 R dry	$\pm 15\%$	$\pm 16\%$	$\pm 20\%$	$\pm 21\%$	6%	+79%	7%
F400 R wet	$\pm 10\%$	$\pm 7\%$	$\pm 9\%$	$\pm 35\%$	3%	+12%	1%
HD3000 R wet	$\pm 15\%$	$\pm 18$	$\pm 22\%$	$\pm 25\%$	7%	+71%	6%
F400 P dry	$\pm 8\%$	$\pm 9\%$	$\pm 7\%$	$\pm 38\%$	4%	+17%	1%
HD3000 P dry	$\pm 12\%$	+10%	+20%	$\pm 25\%$	6%	+101%	2%
F400 P wet	$\pm 10\%$	$\pm 10\%$	$\pm 9\%$	$\pm 37\%$	6%	+18%	1%
HD3000 P wet	$\pm 13\%$	+16%	+16%	$\pm 29\%$	8%	+100%	3%

( $\Delta$  represents the changes of parameters from the untreated (virgin) GAC samples;  $\pm$  values indicate the highest of percent negative or positive difference as compared to untreated GAC samples for each parameter;  $\uparrow$  represents the increase from the untreated GAC samples)

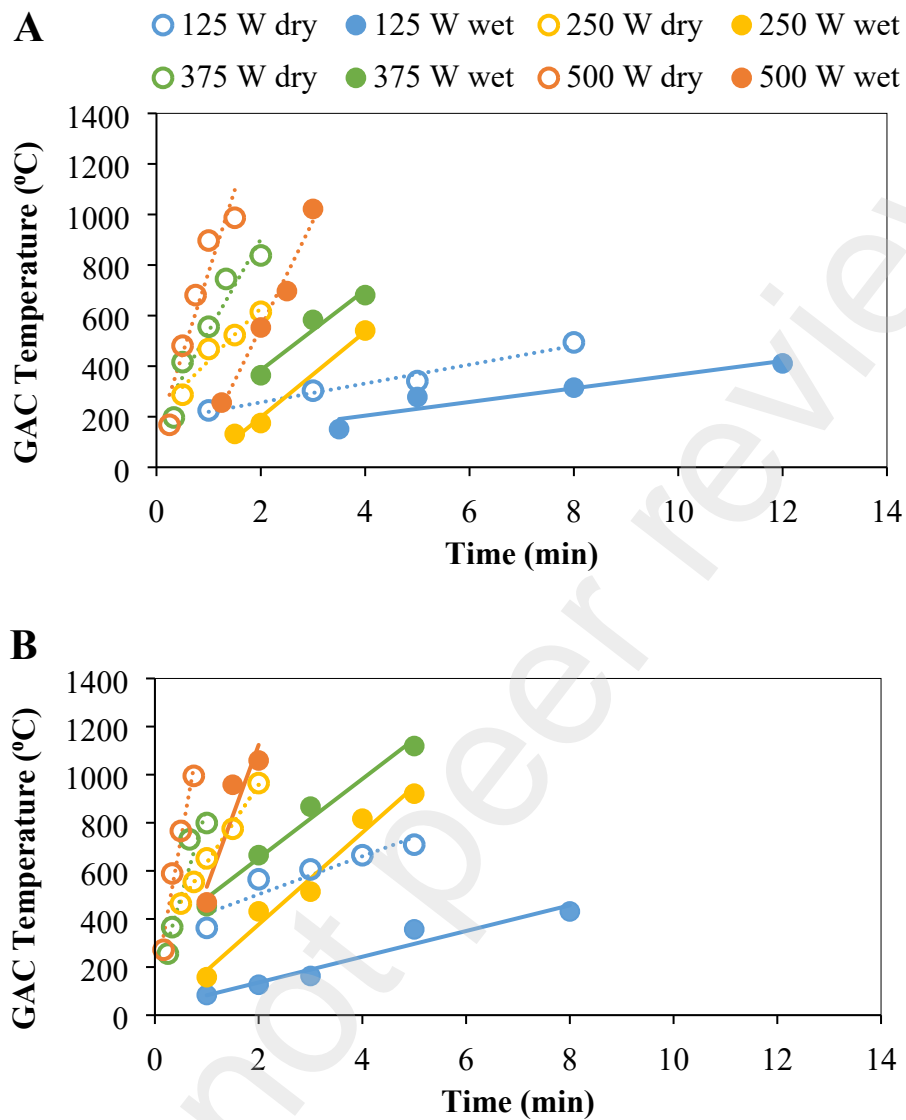


**Figure 1.** MW power and irradiation time dependent temperature profiles of F400 R [A] and F400 P [B] samples under dry and wet conditions. (Solid symbols: wet conditions; open symbols: dry conditions, lines show linear-fit).

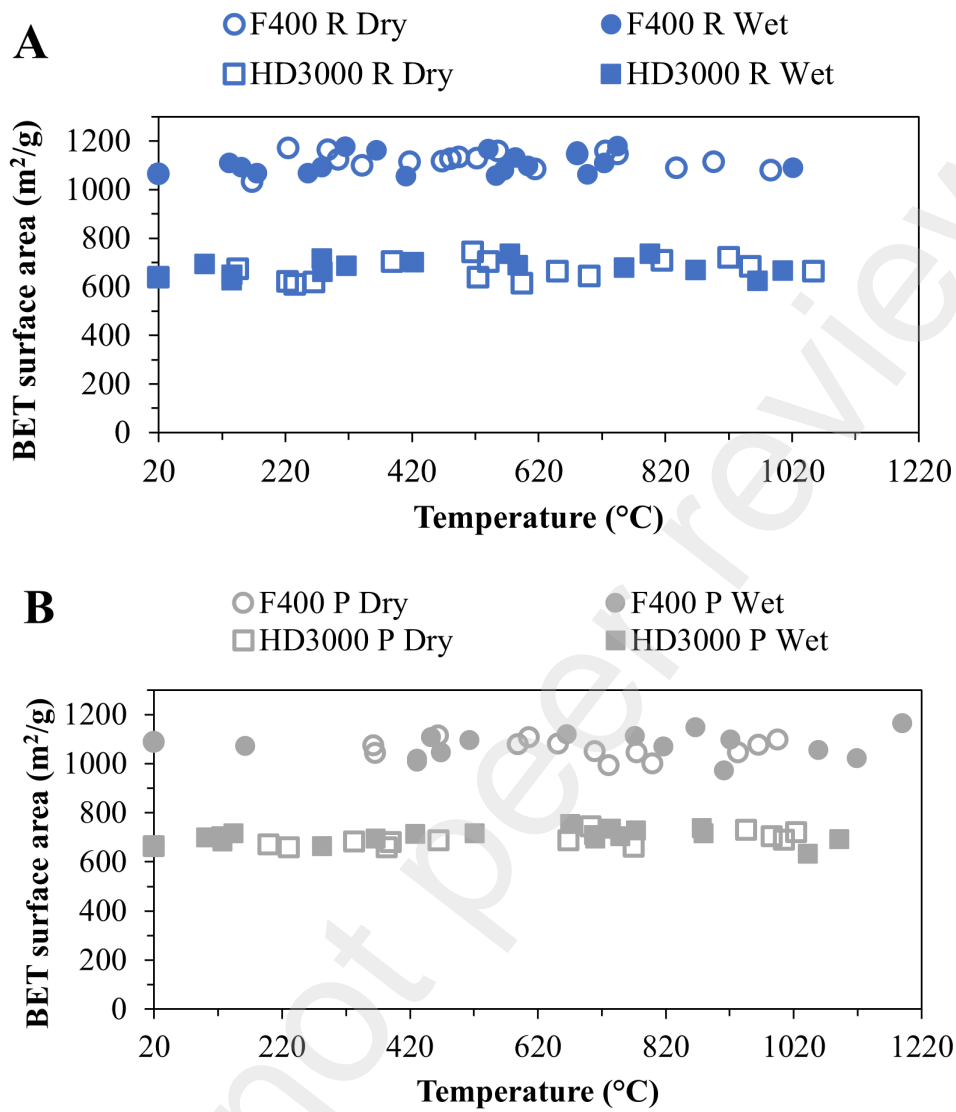


**Figure 2.** Temperature-dependent BET surface area profiles of F400 R and HD3000 R [A] and F400 P and HD3000 P [B] GAC samples under wet and dry conditions upon MW irradiation. (Solid symbols: wet conditions; open symbols: dry conditions)

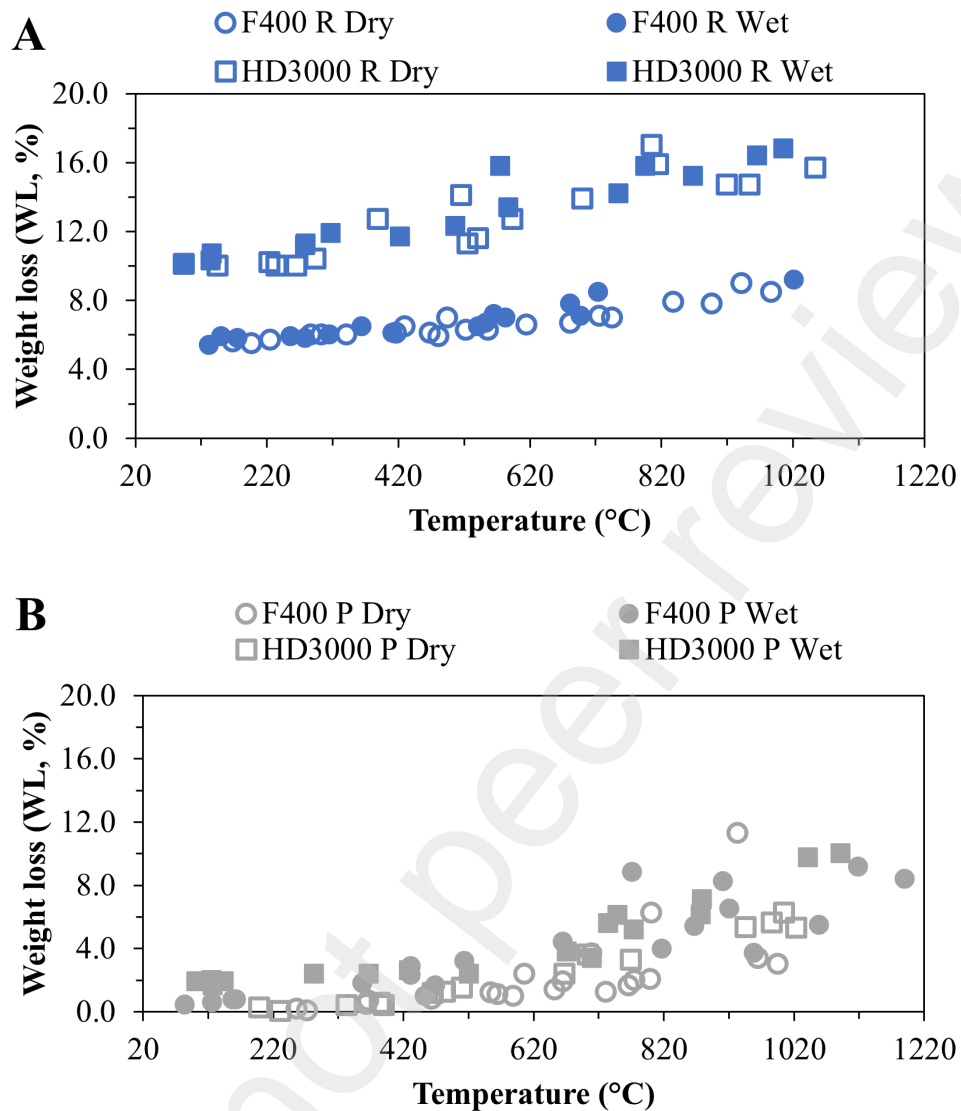


**Figure 3.** Temperature-dependent weight loss profiles of F400 R and HD3000 R [A] and F400 P and HD3000 P [B] GAC samples under wet and dry conditions upon MW irradiation. (Solid symbols: wet conditions; open symbols: dry conditions)

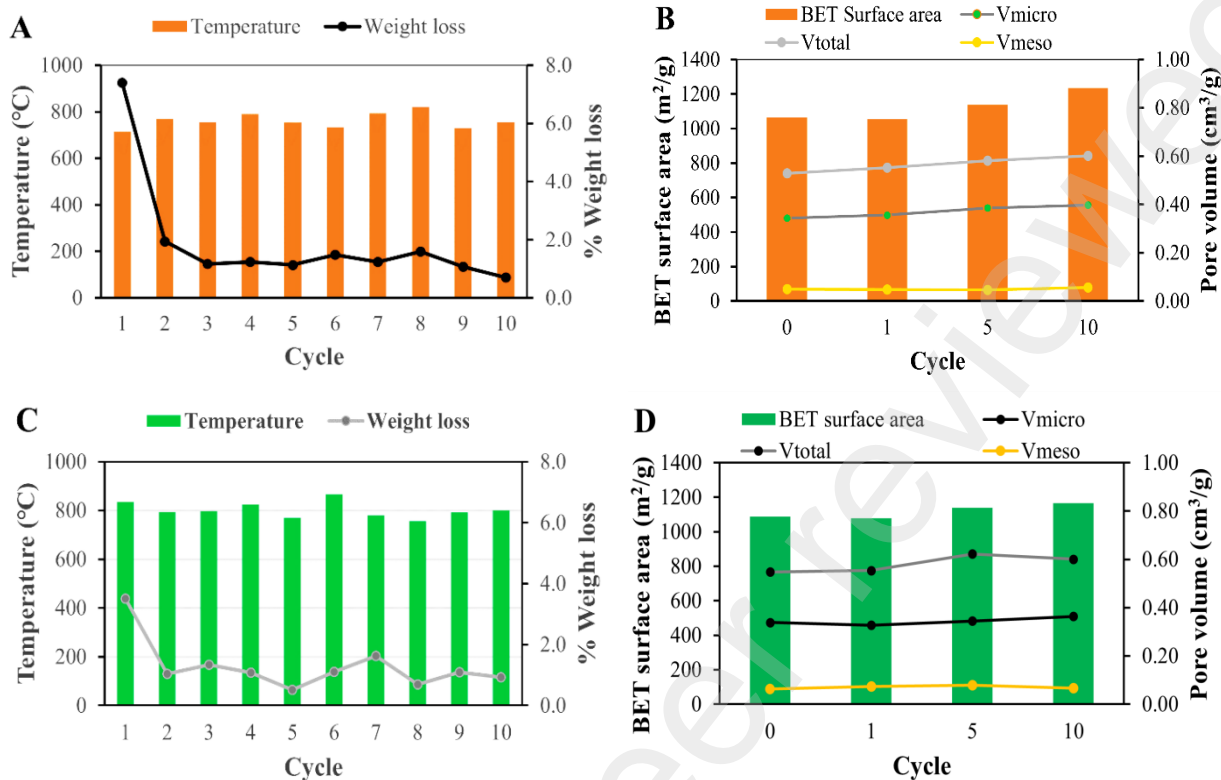


**Figure 4.** The impact of multi-cycle MW irradiation on the physical characteristics of F400 GAC samples under wet condition. Temperature vs % weight loss for F400 R and F400 P in A and C, respectively. BET surface area vs pore volumes (total, micro, and meso) of F400 R and F400 P in B and D, respectively.

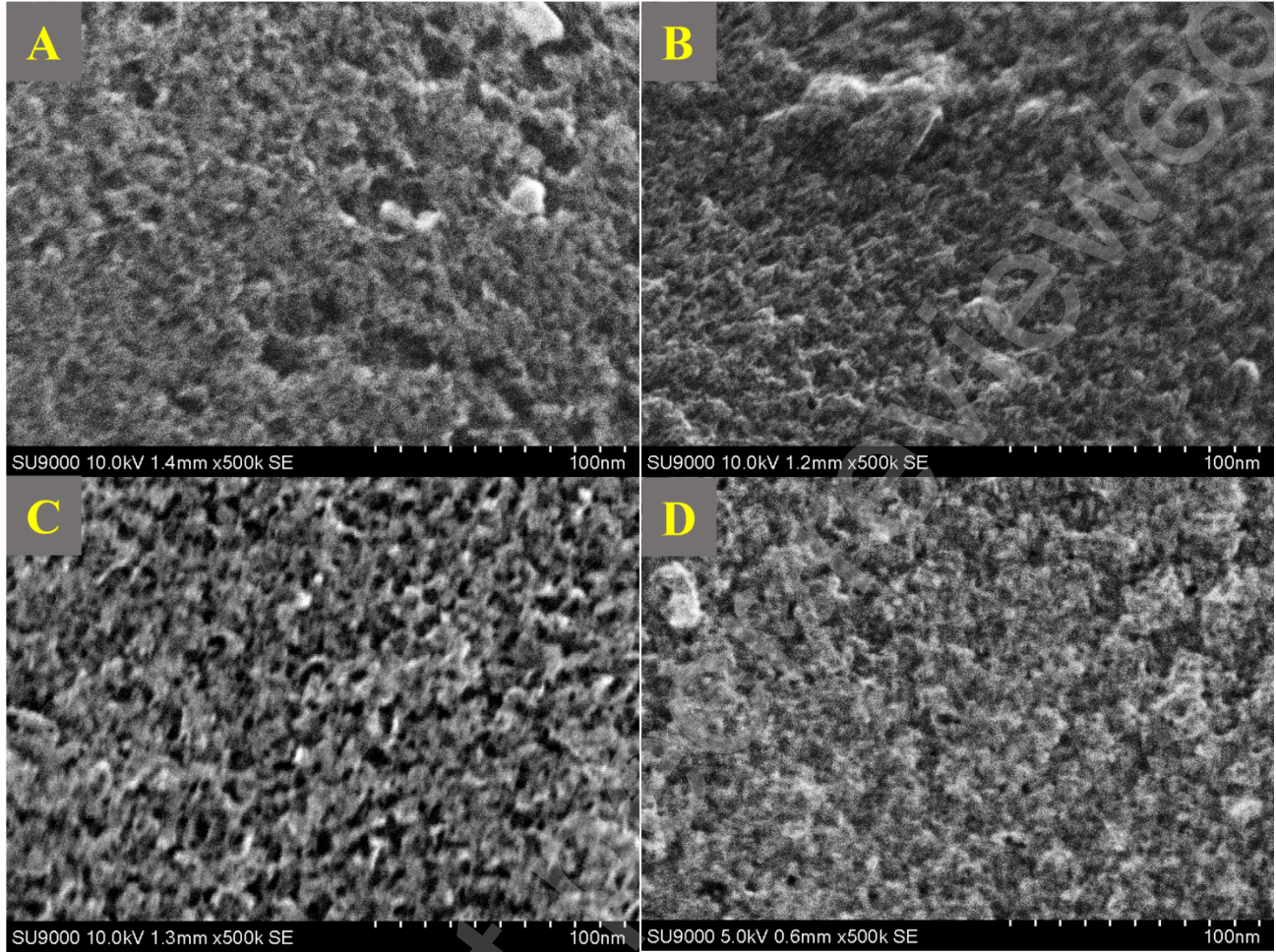


**Figure 5.** SEM images of F400 R samples before and after different cycles of MW irradiation over 600 °C. [A] virgin, [B] one cycle, [C] five cycles, and [D] ten cycles. All images are captured at 500k magnifications.

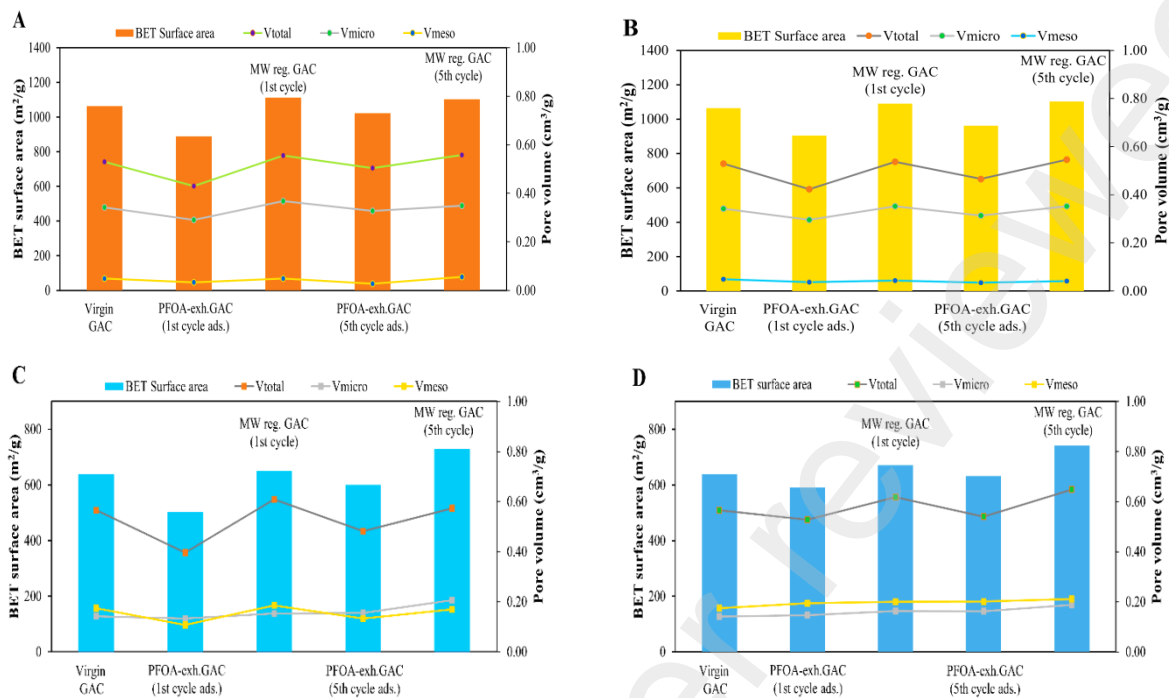


**Figure 6.** The impact of MW irradiation on the GAC BET surface area and pore volumes during multi-cycles MW regeneration of PFOA-loaded F400 ([A] in DDW and [B] in Lake Hartwell water) and HD3000 ([C] in DDW and [D] in Lake Hartwell water).

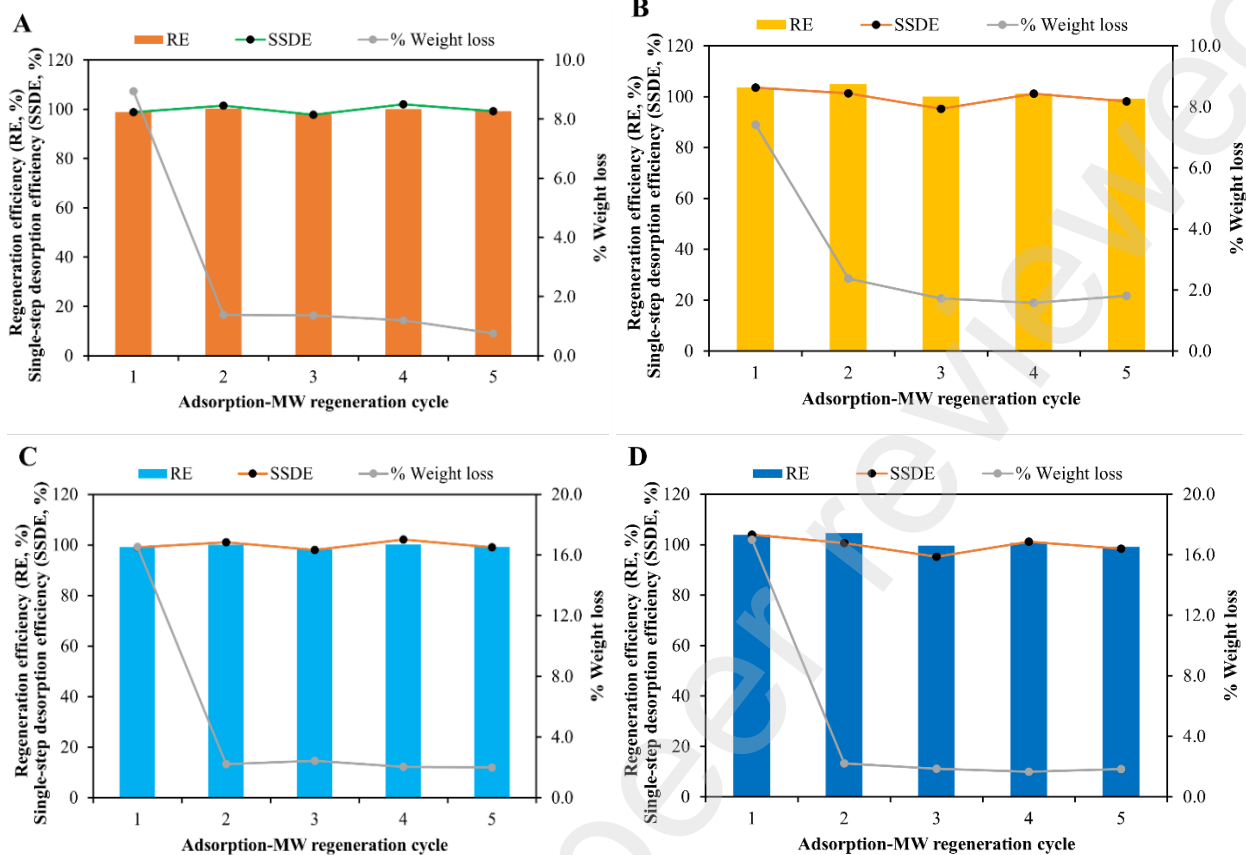


**Figure 7.** GAC adsorption capacity (expressed in terms of regeneration efficiency and single-step desorption efficiency) and weight loss percentage during multi-cycles MW regeneration of PFOA-loaded F400 ([A] in DDW and [B] in Lake Hartwell water) and HD3000 ([C] in DDW and [D] in Lake Hartwell water).